Loop Shaping Control of Distribution STATCOM

Kittaya Somsai[1], Nitus Voraphonpiput[2] and Thanatchai Kulworawanichpong[1*]

[1]*School of Electrical Engineering, Suranaree University of Technology, Nakhon Ratchasima, Thailand*
[2]*Power Purchase Division, Electric Generating Authority of Thailand, Bangkok, Thailand*
** Corresponding Author, e-mail: thanatchai@gmail.com*

Abstract

This paper presents the system modeling and control design for the load voltage regulation using distribution static compensators (D-STATCOMs). The decoupling control based on the dq reference frame with the symmetrical optimum method is applied to design the D-STATCOM current and DC voltage controllers. The modeling strategy similar to that used for the field-oriented control of three-phase AC machines is employed to model the distribution system integrating with the D-STATCOM and its control circuit. This derived model is used for the load voltage controller design based on the linearized technique, called classical loop shaping method. A simplified 11-kV, 2-bus test power system is employed for simulation. Satisfactory results obtained by simulating the proposed model are compared with those obtained by the switching control of D-STATCOM power circuit created in MATLAB's Power System Blockset. As a result, the effectiveness of proposed model is verified. This design gave satisfactory responses to guarantee at least 3 dB of the gain margin and 40° of the phase margin.

Keywords: *D-STATCOM, voltage regulation, decoupling control, symmetrical optimum, classical loop shaping*

1. Introduction

In a power distribution system, voltage sag contributes more than 80% of power quality (PQ) problems that exist in power systems [1–2]. It is caused by a fault in the utility system, a fault within the customer's facility or a large increase of the load current, like starting a motor or transformer energizing, operation of process controllers; programmable logic controllers (PLC), adjustable speed drive (ASD) and robotics [1], and used of high intensity discharge lamps [3].

Controlled reactive power sources are commonly used for load voltage regulation in presence of disturbances like voltage sag. Due to their high control bandwidth, D-STATCOMs, based on three-phase pulse width modulation voltage source converters, have been proposed for this application [3–7]. For a fast control, the D-STATCOM is usually modeled using the *dq* axis theory for balanced three-phase systems, which allows definition of instantaneous reactive current and instantaneous magnitude of phase voltages [8]. In addition, the current controller design is developed using a rotating *dq* frame of reference that offers higher accuracy than the stationary frame techniques [9].

Most literatures on the D-STATCOM and STATCOM control concentrates in control of the output current and DC voltage regulation for a given reactive current reference. The current decoupling control based on the *dq* reference frame received considerable attention in [10–12]. To alleviate the interaction between the active and reactive currents, a feed-forward control loop with reactive current deviations as the input was introduced to compensate for the DC voltage drop [13]. In addition, an alternative approach using a linearized state space model in the D-STATCOM and STATCOM control design was proposed in [14–15]. For control design, a small signal model of the distribution system was derived by transforming the equivalent system impedance to the *dq* frame rotating at the power frequency in steady state, thereby imposing a limitation on the dynamic response [16].

In this paper, the D-STATCOM current and DC voltage decoupling control based on the *dq* reference frame are used and the proportional gain and integral time of PI controllers are also with its design. This derived model is used for the load voltage controller design based on some linearized technique, called classical loop shaping method. By using MATLAB for adjusting the transfer function to satisfy the loop shaping specifications, the controller's parameters and the stability margins for an inductive *RL* load with various operating conditions can be obtained. Performance of the proposed model and the controller design were verified using computer simulation performed in SIMULINK/MATLAB. In addition, the simulation results of the proposed model and the PSB in SIMULINK/MATLAB are compared in order to verify the proposed model.

2. Modeling of Power Distribution Systems

The system considered here is a simplified model of a load served by an electric power distribution system. The D-STATCOM is connected in parallel with the load. The distribution system with the D-STATCOM and its per-phase equivalent circuit are shown in Figure 1 and Figure 2, respectively. The system consists of the source modeled as an infinite bus with inductive source impedance, the load modeled by a series RL circuit, the D-STATCOM modeled as a controllable current source, and coupling capacitor. The coupling capacitor is used as a harmonic filter or fixed compensation capacitors connected in parallel with the load.

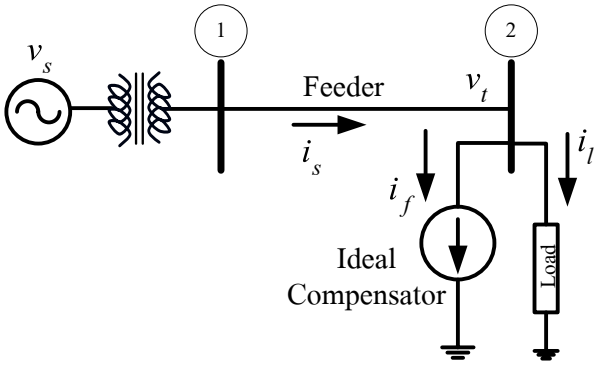

Figure 1. Distribution System with D-STATCOM

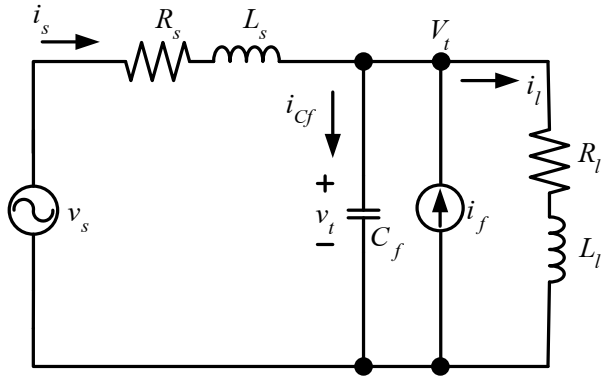

Figure 2. Per-phase Equivalent Circuit

2.1. Modeling with an Inductive *RL* Load

For an inductive load, *RL* load, it assumes that the source, the load and the D-STATCOM are balanced. Hence, the system dynamics can be described as:

$$L_s \frac{di_{s,abc}}{dt} = -R_s i_{s,abc} - v_{t,abc} + v_{s,abc} \quad (1)$$

$$C_f \frac{dv_{t,abc}}{dt} = -\frac{v_{t,abc}}{R_l} + i_{s,abc} + i_{f,abc} \quad (2)$$

Here, $i_{s,abc}$, $i_{f,abc}$, $v_{s,abc}$ and $v_{t,abc}$ are vectors consisting of individual phase quantities denoted in Figure 2, R_l is a load resistance, X_l is a load reactance, L_s is a source inductance, R_s is a source resistance, and C_f is a coupling capacitor. Under the assumption that zero sequence components are not presented, (1) – (2) can be transformed to an equivalent two-phase system by applying the following three-to-two phase transformation:

$$v_{s,xy} = v_{sa}e^{j0} + v_{sb}e^{j2\pi/3} + v_{sc}e^{j4\pi/3} \quad (3)$$

Where the complex number, $v_{s,xy} \triangleq v_{sx} + jv_{sy}$. This is followed by the following rotational transformation:

$$v_{s,dq} \triangleq v_{sd} + jv_{sq} = e^{-j\theta}v_{s,xy} \quad (4)$$

Applying the transformations, (1) – (2) can be written as:

$$C_f \dot{v}_{td} = -i_{ld} + \omega C_f v_{tq} + i_{sd} + i_{fd} \quad (5)$$

$$C_f \dot{v}_{tq} = -i_{lq} - \omega C_f v_{td} + i_{sq} + i_{fq} \quad (6)$$

$$L_l \dot{i}_{ld} = -R_l i_{ld} + \omega L_l i_{lq} + v_{td} \quad (7)$$

$$L_l \dot{i}_{lq} = -R_l i_{lq} - \omega L_l i_{ld} + v_{tq} \quad (8)$$

Where $\omega \triangleq \frac{d\theta}{dt}$ is to be designed and also be a function of time.

2.2. Choice of the Reference Frame

We choose the dq reference frame which is similar to that used for field-oriented control of three phase AC machines. Thus, angle θ used in (4) is defined by $\theta = \tan^{-1}(v_{ty}/v_{tx})$. This implies that

$$v_{tq} \equiv 0 \;\rightarrow\; \dot{v}_{tq} = 0 \tag{9}$$

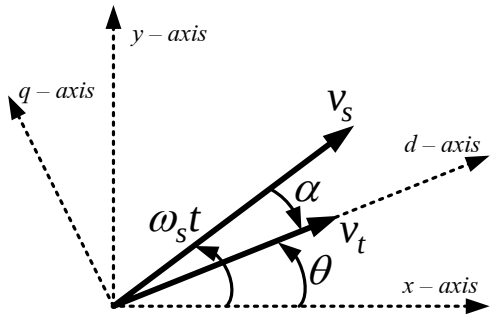

Figure 3. Orientation of Reference Frames

Defining $\alpha = \theta - \omega_s t$, where ω_s is the power frequency, we get $v_{s,dq} = V_s.e^{-j\alpha}$, where V_s is the magnitude of the supply voltage. The relative orientation of the vectors $v_{t,dq}$, $v_{s,dq}$ and the reference frame are shown in Figure 3. The system equations for the *RL* load can now be rewritten as:

$$L_s\dot{i}_{sd} = -R_s i_{sd} + \omega L_s i_{sq} - v_{td} + V_s \cos\alpha \tag{10}$$
$$L_s\dot{i}_{sq} = -R_s i_{sq} - \omega L_s i_{sd} - V_s \sin\alpha \tag{11}$$
$$C_f\dot{v}_{td} = -i_{ld} + i_{sd} + i_{fd} \tag{12}$$
$$L_l\dot{i}_{ld} = -R_l i_{ld} + \omega L_l i_{lq} + v_{td} \tag{13}$$
$$L_l\dot{i}_{lq} = -R_l i_{lq} - \omega L_l i_{ld} \tag{14}$$
$$\dot{\alpha} = \omega - \omega_s \tag{15}$$
$$\omega = \frac{-i_{lq}+i_{sq}+i_{fq}}{C_f v_{td}} \tag{16}$$

Where (16) is derived by using (9). This should be note that ω varies with time and is different from ω_s. Since $v_{tq} \equiv 0$, v_{td} represents the instantaneous magnitude of the phase voltages $v_{t,abc}$, while i_{fq} denotes the instantaneous reactive current supplied by the D-STATCOM. In addition, in the absence of negative sequence components, all the state variables in (10) – (15) is constant in steady state. Thus, this balanced three-phase system is effectively transformed into an equivalent DC system and its control problem is therefore simplified. (16) defines ω for the *RL* load. Thus, (10) – (16) define the system which can be used to design a controller.

3. D-STATCOM Modeling and Control

3.1. D-STATCOM Modeling

The basic circuit diagram and control of the D-STATCOM system are shown in Figure 4. It consists of a three-phase voltage source converter (VSC), an interfacing inductor, a DC link capacitor, and its control system. The VSC is connected to the network through a transformer and the interfacing inductor which are also used to filter high-frequency components of compensating currents. The inductance L_f in this figure represents the leakage inductance of the transformer and the interfacing inductor. The switching losses of the converter and the copper losses of the transformer are represented by a resistance R_f. In this paper, the D-STATCOM is used for load voltage regulation by injecting appropriate reactive power. Therefore, the control systems of the D-STATCOM consist of current control, DC voltage control, and AC voltage control. The primary control objective is to rapidly regulate the reactive current i_{fq} to the reference value (i_{fq}^*) which is generated by a load voltage controller. A secondary control objective is to keep the DC voltage at a desired value. It assumes that the internal dynamics of the D-STATCOM are slower than the switching period of the converter [16], so the D-STATCOM dynamics can be written as:

$$L_f \frac{di_{f,abc}}{dt} = -R_f i_{f,abc} - v_{t,abc} + v_{st,abc} \tag{17}$$

$$C_{dc}\dot{v}_{dc} = -\frac{v_{dc}}{R_d} - v_{st,abc}^T i_{f,abc} \tag{18}$$

Here, v_{dc} is the D-STATCOM's DC voltage, v_{st} is the D-STATCOM's output AC voltage, i_f is the D-STATCOM's output current, v_t is the load voltage, while the subscript "abc" implies three-phase vectors consisting of individual phase quantities. Parameters in these equations are DC link capacitance, C_{dc}, and capacitor leakage resistance, R_d. After applying the three-phase to two-phase transformation given by (3) followed by the rotational transformation of (4), the D-STATCOM dynamics can be rewritten as:

$$L_f \dot{i}_{fd} = -R_f i_{fd} + \omega L_f i_{fq} - v_{td} + k_p u_d v_{dc} \tag{19}$$

$$L_f \dot{i}_{fq} = -R_f i_{fq} - \omega L_f i_{fd} + k_p u_q v_{dc} \tag{20}$$

$$C_{dc}\dot{v}_{dc} = -\frac{v_{dc}}{R_d} - \frac{3}{2}k_p u_d i_{fd} - \frac{3}{2}k_p u_q i_{fq} \tag{21}$$

Where ω has been previously defined in (16), v_{dc}, i_{fd} and i_{fq} represent the state variables of the D-STATCOM, k_p is a constant value depending on the type of converters and transformer ratio, while u_d and u_q are the control inputs.

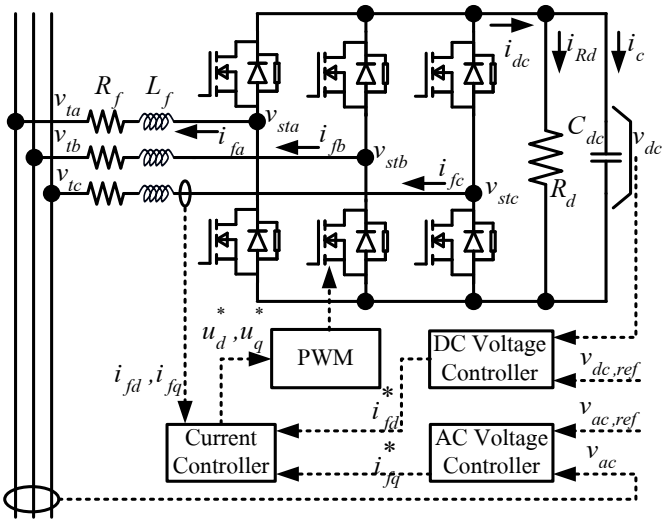

Figure 4. Basic Circuit Diagram and Control of the D-STATCOM System

3.2. D-STATCOM Modeling

The equations in (19) and (20) are used for designing the D-STATCOM current controller. These equations clearly show that the D-STATCOM output currents are induced by its output voltage modulation. However, the current control of the converter on the *dq* reference frame is a two-input two-output system with cross coupling between active and reactive currents. To eliminate the cross coupling effect, a decoupling control based on the *dq* reference frame is introduced where the proportional-plus-integral (PI) regulators are used to control the D-STATCOM currents in this work. The current control structure for the D-STATCOM and the D-STATCOM output current are detailed in Figure 5. The D-STATCOM output AC voltage, v_{st}, is generated by the VSC with pulse width modulation (PWM) and the D-STATCOM output voltage commands, u_d^* and u_q^*, are the inputs. The VSC with PWM can be simplified as $\frac{k_p v_{dc}}{sT_d+1}$ where T_d is the dead time.

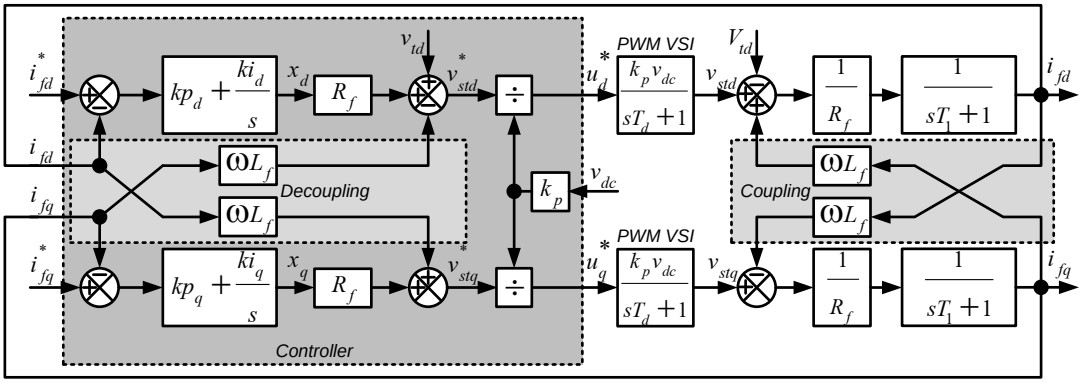

Figure 5. Current Control Structure for the D-STATCOM

3.3. DC Voltage Control (DC Link Voltage Control)

The secondary control objective is to keep v_{dc} around its reference. This objective cannot be achieved directly by u_d through (21) as there might be possibility of i_{fd} going to zero during a transient. However, v_{dc} can be controlled indirectly by adjusting i_{fd}. For designing the DC voltage controller, (21) is used. Although, v_{dc} can be controlled by varying i_{fd}, i_{fq} still affects v_{dc} through $u_q i_{fq}$ of (21). To eliminate this effect, the controller with decoupling, $u_q i_{fq}$, is applied where the proportional-plus-integral (PI) regulators are used to control the DC voltage. The DC voltage control structure and the D-STATCOM DC voltage are demonstrated in Fig. 6. The active current command i_{fd}^*, accounting for the DC voltage regulation, can be generated by the DC voltage controller with the DC voltage deviation as its input. The i_{fd}^* is used as the input of the current control, $G_{c,i}(s)$, then the controlled active current results in the regulation of the D-STATCOM's DC link voltage.

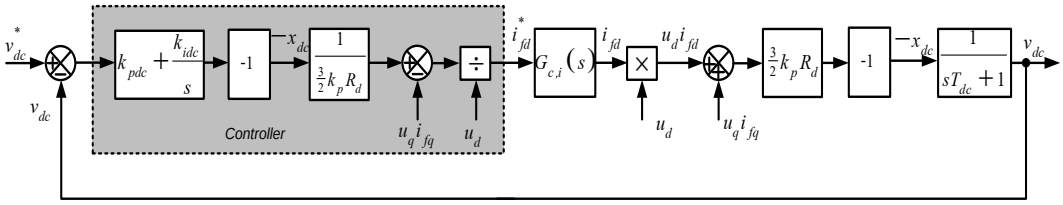

Figure 6. DC Voltage Control Structure and the D-STATCOM dc Voltage

The PI controller parameters depend on the parameters of the closed-loop transfer function, natural frequency (ω_0), damping coefficient (ζ), and pole value (p). In general, ω_0 and ζ characterize the desired system behavior and they are fixed, while the pole value can be chosen. Specific pole values can be imposed by using supplementary conditions. In this paper, the conditions for choosing the pole value refer to the symmetrical optimum method that is described in [17] and [18], which simplify expressions of the PI parameters. The goal is to find the pole value of the closed-loop transfer function which satisfies the assumptions of the symmetrical optimum method around ω_0 for the transfer function of the open-loop system.

4. Load Voltage Control using the Loop Shaping Method

Based on the distribution system model described in the previous section, we are now to design the load voltage controller. In addition, the D-STATCOM model and its control were integrated with the power distribution system for designing the load voltage controller. From the current control with decoupling as shown in Figure 5, the control inputs, u_d and u_q, of the D-STATCOM dynamics in (19) – (21) can be written as:

$$u_d = \frac{1}{k_p v_{dc}}\left[kp_d R_f\left(i_{fd}^* - i_{fd}\right) + ki_d R_f f_d - \omega L_f i_{fq} + v_{td}\right] \quad (22)$$

$$u_q = \frac{1}{k_p v_{dc}}\left[kp_q R_f\left(i_{fq}^* - i_{fq}\right) + ki_q R_f f_q + \omega L_f i_{fd}\right] \quad (23)$$

While the active current command i_{fd}^{*} can be derived from the DC voltage control with decoupling as shown in Figure 6 as:

$$i_{fd}^{*} = \frac{1}{u_d}\left[\frac{-kp_{dc}}{\frac{3}{2}k_p R_d}(v_{dc}^{*} - v_{dc}) - \frac{ki_{dc}}{\frac{3}{2}k_p R_d}v_d - u_q i_{fq}\right] \tag{24}$$

Where $\omega L_f i_{fq}$, $\omega L_f i_{fd}$ and $u_q i_{fq}$ are the decoupling terms of the current control and the DC voltage control, respectively. In addition, the dynamic equations of the current control and the DC voltage control that were integrated with the system can be written as:

$$\dot{f}_d = i_{fd}^{*} - i_{fd} \tag{25}$$

$$\dot{f}_q = i_{fq}^{*} - i_{fq} \tag{26}$$

$$\dot{v}_d = v_{dc}^{*} - v_{dc} \tag{27}$$

Therefore, the distribution system model in (10) – (16), the D-STATCOM dynamics in (19) – (21) and the dynamic equations of the D-STATCOM controllers in (22) – (27) can be used to form a set of state equations to design the load voltage controller for the *RL* load. For designing the load voltage controller, the load voltage v_{td} is chosen as the output of the system with the reactive current command i_{fq}^{*} as the control input. However, these state equations are a set of nonlinear differential equations. To investigate the dynamic performance of these systems, linear approximation is applied. Linearization of these systems around a specified operating point that described in [19] gives a set of linear equations for the inductive *RL* load as shown in (28).

$$\frac{d}{dt}\begin{bmatrix}\Delta v_{td}\\ \Delta i_{sd}\\ \Delta i_{sq}\\ \Delta i_{fd}\\ \Delta i_{fq}\\ \Delta v_{dc}\\ \Delta\alpha\\ \Delta f_d\\ \Delta f_q\\ \Delta v_d\\ \Delta i_{ld}\\ \Delta i_{lq}\end{bmatrix} = \begin{bmatrix} 0 & k_{isd1} & 0 & k_{ifd1} & 0 & 0 & 0 & 0 & 0 & 0 & k_{ild1} & 0\\ k_{vtd2} & k_{isd2} & k_{isq2} & 0 & k_{ifq2} & 0 & k_{\alpha 2} & 0 & 0 & 0 & 0 & k_{ilq2}\\ k_{vtd3} & k_{isd3} & k_{isq3} & 0 & k_{ifq3} & 0 & k_{\alpha 3} & 0 & 0 & 0 & 0 & k_{ilq3}\\ k_{vtd4} & 0 & k_{isq4} & k_{ifd4} & k_{ifq4} & k_{vdc4} & 0 & k_{fd4} & k_{fq4} & k_{vd4} & 0 & k_{ilq4}\\ 0 & 0 & 0 & 0 & k_{ifq5} & 0 & 0 & 0 & k_{fq5} & 0 & 0 & 0\\ k_{vtd6} & 0 & k_{isq6} & k_{ifd6} & k_{ifq6} & k_{vdc6} & 0 & k_{fd6} & k_{fq6} & k_{vd6} & 0 & k_{ilq6}\\ k_{vtd7} & 0 & k_{isq7} & 0 & k_{ifq7} & 0 & 0 & 0 & 0 & 0 & 0 & k_{ilq7}\\ 0 & 0 & k_{isq8} & k_{ifd8} & k_{ifq8} & k_{vdc8} & 0 & 0 & k_{fq8} & k_{vd8} & 0 & k_{ilq8}\\ 0 & 0 & 0 & 0 & k_{ifq9} & 0 & 0 & 0 & 0 & 0 & 0 & 0\\ 0 & 0 & 0 & 0 & 0 & k_{vdc10} & 0 & 0 & 0 & 0 & 0 & 0\\ k_{vtd11} & 0 & k_{isq11} & 0 & k_{ifq11} & 0 & 0 & 0 & 0 & 0 & k_{ild11} & k_{ilq11}\\ k_{vtd12} & 0 & k_{isq12} & 0 & k_{ifq12} & 0 & 0 & 0 & 0 & 0 & k_{ild12} & k_{ilq12}\end{bmatrix}\begin{bmatrix}\Delta v_{td}\\ \Delta i_{sd}\\ \Delta i_{sq}\\ \Delta i_{fd}\\ \Delta i_{fq}\\ \Delta v_{dc}\\ \Delta\alpha\\ \Delta f_d\\ \Delta f_q\\ \Delta v_d\\ \Delta i_{ld}\\ \Delta i_{lq}\end{bmatrix} + \begin{bmatrix}0\\0\\0\\b_{ifd}\\b_{ifq}\\b_{vdc}\\0\\b_{fd}\\b_{fq}\\0\\0\\0\end{bmatrix}\Delta i_{fq}^{*} \tag{28}$$

Table 1. Parameters of the Power Distribution System and the D-STATCOM

Distribution power system parameters	
Nominal source voltage (V_s)	12.81 *kV*
Desired load voltage magnitude (v_{td}^*)	11.00 *kV*
Source resistance and inductance (R_s and L_s)	1 Ω and 10 *mH*
Load resistance and inductance (R_l and L_l)	10 Ω and 10 *mH*
System frequency (f_s)	50 *Hz*
D-STATCOM parameters	
Coupling capacitor (C_f)	50 μF
Interfacing resistance and inductance (R_f and L_f)	0.1 Ω and 10 *mH*
Constant value of converter (k_p)	0.55
DC link voltage (v_{dc})	30 *kV*
DC link capacitance (C_{dc})	200 μF
Capacitor leakage resistance (R_d)	61.273 *k*Ω
Switching frequency (f_{sw})	10 *kHz*

Base on the parameters of the distribution system and the D-STATCOM as shown in Table 1 and the D-STATCOM controllers as described in the previous section, the operating points of the systems can be obtained as shown in Table 2. Bode plots of the transfer function $\frac{\Delta v_{td}(s)}{\Delta i_{fq}^*(s)}$ for the linearized system of (28) with the operating point as shown in Table 2 is shown in Figure 7.

Table 2. Operating Points of the System

$V_s\ (kV)$	12.81 (1.0 pu.)	11.53 (0.9 pu.)	10.25 (0.8 pu.)	8.97 (0.7 pu.)
$i_{fq0}\ (A)$	0	-463.22	-960.10	-1516.0
$v_{td0}\ (kV)$	11.00	11.00	11.00	11.00
$i_{sd0}\ (A)$	1002.08	1004.03	1010.46	1022.98
$i_{sq0}\ (A)$	-143.97	321.48	818.35	1374.25
$i_{fd0}\ (A)$	-0.89	-2.84	-9.27	-21.79
$v_{dc0}\ (kV)$	30	30	30	30
$\alpha_0\ (red)$	-0.237	-0.306	-0.400	-0.537
$f_{d0}\ (A)$	0	0	0	0
$f_{q0}\ (A)$	0	0	0	0
$v_{d0}\ (kV)$	0	0	0	0
$i_{ld0}\ (A)$	1001.19	1001.19	1001.19	1001.19
$i_{lq0}\ (A)$	-314.53	-314.53	-314.53	-314.53

The bode plots of the transfer function for various operating conditions corresponding to a different value of i_{fq}, are also shown in Figure 7. Remarkably, the system dynamic in (28) gives non-minimum phase.

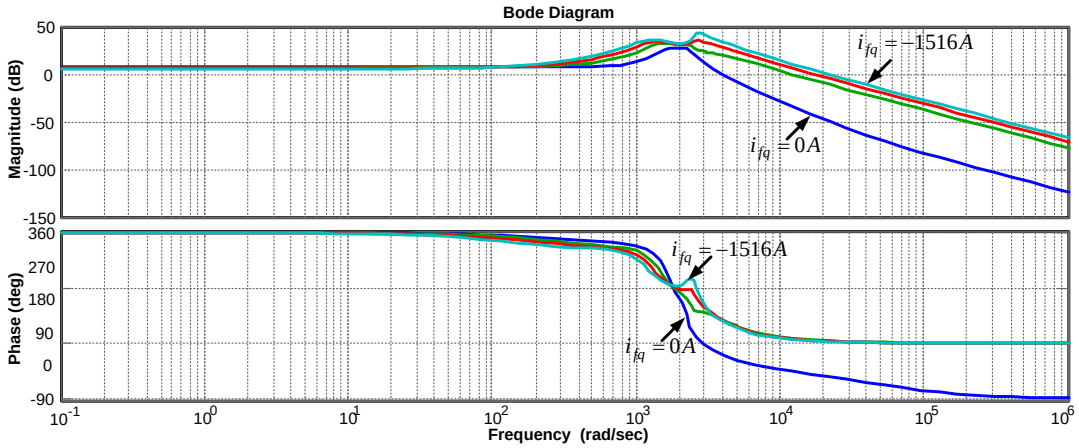

Figure 7. Bode Plots of the Transfer Function $\frac{\Delta v_{td}(s)}{\Delta i^{*}_{fq}(s)}$

4.1. Linear Controller Design using the Loop Shaping Method

The load voltage control is a single-input, single-output (SISO) control system with the load voltage v_{td} chosen as the output of the system and the reactive current command i^{*}_{fq} as the control input. For SISO systems, the classical loop shaping concept is a basis for designing the load voltage controller. The unity-feedback SISO system is depicted in Figure 8 where $P(s)$ represents the plant transfer function and $C(s)$ represents the controller transfer function. The signals $r(t)$, $d_i(t)$, $d_o(t)$, and $n(t)$ are reference input, input disturbance, output disturbance, and sensor noise, respectively. The signal $y(t)$ is the output, $e(t)$ is the tracking error, and $u(t)$ is the control input. The definitions of the open-loop transfer function $L(s)$, the sensitivity function $S(s)$, and the complementary sensitivity function $T(s)$ are:

$$L(s) = P(s)C(s) \tag{29}$$
$$S(s) = [1 + L(s)]^{-1} \tag{30}$$
$$T(s) = L(s)[1 + L(s)]^{-1} \tag{31}$$

The classical loop shaping is a design procedure that explicitly involves the shaping or the adjustment of the magnitude or loop-gain of the open-loop transfer function, $L(s)$, within a desired frequency spectrum. There are three basic types of loop shaping specifications, which are imposed in a different frequency [20]. i) At low frequencies we require $|L(j\omega)|$ to be large, so that $|S(j\omega)|$ is small and $T(j\omega) \approx 1$. This ensures good command tracking, and low sensitivity to plant variations, two of the most important benefits of the feedback. ii) At high frequencies we require $|L(j\omega)|$ to be small, so that $|T(j\omega)|$ is small. This ensures that the output $y(t)$ will be relatively insensitive to the sensor noise $n(t)$, and that the system will remain closed-loop stable in the appearance of plant variations at these frequencies. iii) $L(j\omega)$

should not drop-off too quickly near the crossover frequency to avoid internal instability. The specifications for the load voltage control performance in this paper are as follow:

1) Zero steady state tracking error.

2) At least 40 dB of disturbance rejection at low frequency.

3) The output $y(t)$ must be relatively insensitive to the sensor noise $n(t)$ at high frequency.

4) The gain margin should be greater than 3 dB and the phase margin should be greater than 40°.

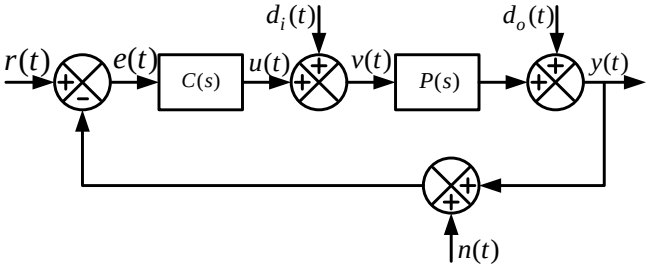

Figure 8. Block Diagram of a Unity Feedback SISO System

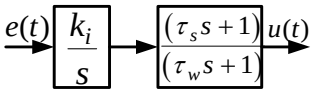

Figure 9. Designed Controller for the Load Voltage Control

Table 3. Controller Parameters and the Stability Margins

5.1) Current and DC voltage control without decoupling			
$v_s\ (kV)$	11.53	10.25	8.97
$i_{fq}\ (A)$	-463	-960	-1516
$v_{td}\ (kV)$	11.00	11.00	11.00
k_i	110	70	50
τ_s	0.00024	0.00024	0.00024
τ_w	0.002	0.002	0.002
GM(dB)	6.75	5.26	4.43
PM(deg)	41.2	42.5	45.0

5.2) Current and DC voltage control with decoupling			
$v_s\ (kV)$	11.53	10	8.97
$i_{fq}\ (A)$	-463	-960	-1516
$v_{td}\ (kV)$	11.00	11.00	11.00
k_i	110	70	50
τ_s	0.00024	0.00024	0.00024
τ_w	0.002	0.002	0.002
GM(dB)	5.94	4.31	3.68
PM(deg)	42.0	44.9	49.2

To satisfy the specifications 1) and 2) requires an integral action in the controller. In addition, the load voltage control gives non-minimum phase, so that the lag compensator is used for satisfying the specifications 3) and 4). The designed controller for the load voltage control is shown in Figure 9. By using MATLAB for adjusting the open-loop transfer function, $L(j\omega)$, to satisfy the loop shaping specifications described above, the controller parameters and the stability margins for the inductive *RL* load with various operating conditions corresponding to a different value of i_{fq} are obtained and presented in Table 3. The bode plots of the plant, desired controller, and the open-loop system including the plant augmented with the desired controller when the source voltage is 0.7 per-unit are demonstrated in Figure 10 whereas the root locus of the closed-loop system are shown in Figure 11.

In Figure 10, the bode plots for the inductive *RL* load, shows that $|L(j\omega)|$ is greater than 40 dB at low frequency while at high frequency, $|L(j\omega)|$ is small. The gain margin of the control loop is 3.68 dB at 487 rad/s and the phase margin is 49.2° at 122 rad/s, therefore specifications 1) – 4) are satisfied. In accordance with the root locus of the closed-loop system shown in Figure 11, all the closed-loop poles are on the left-half of the complex plane (LHP). Thus, the closed-loop system of the inductive *RL* load is stable.

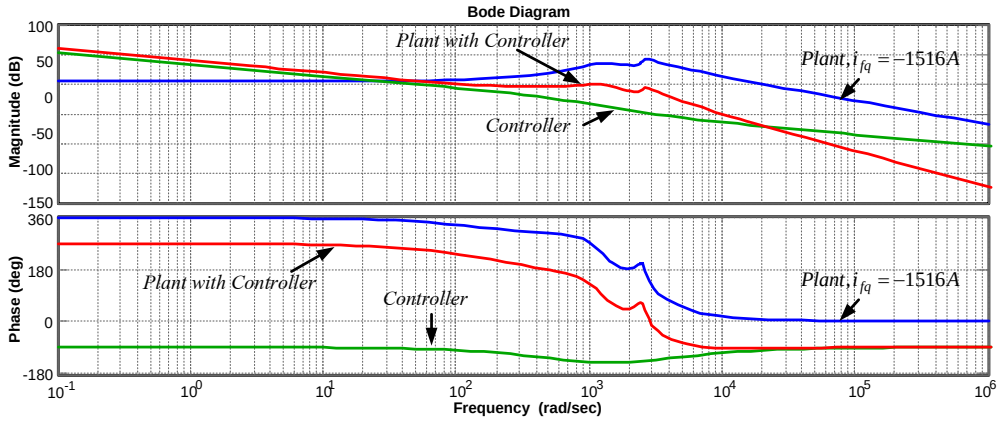

Figure 10. Open-loop System Including the Plant with the Desired Controller

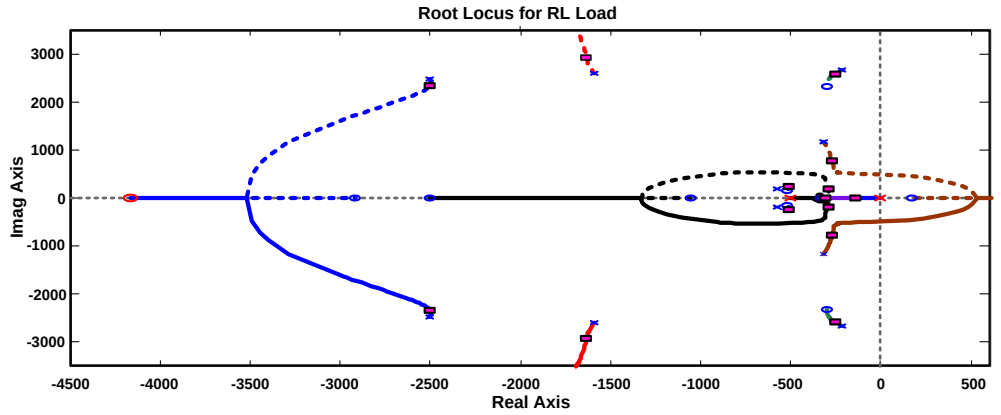

Figure 11. Root Locus of the Closed-loop System

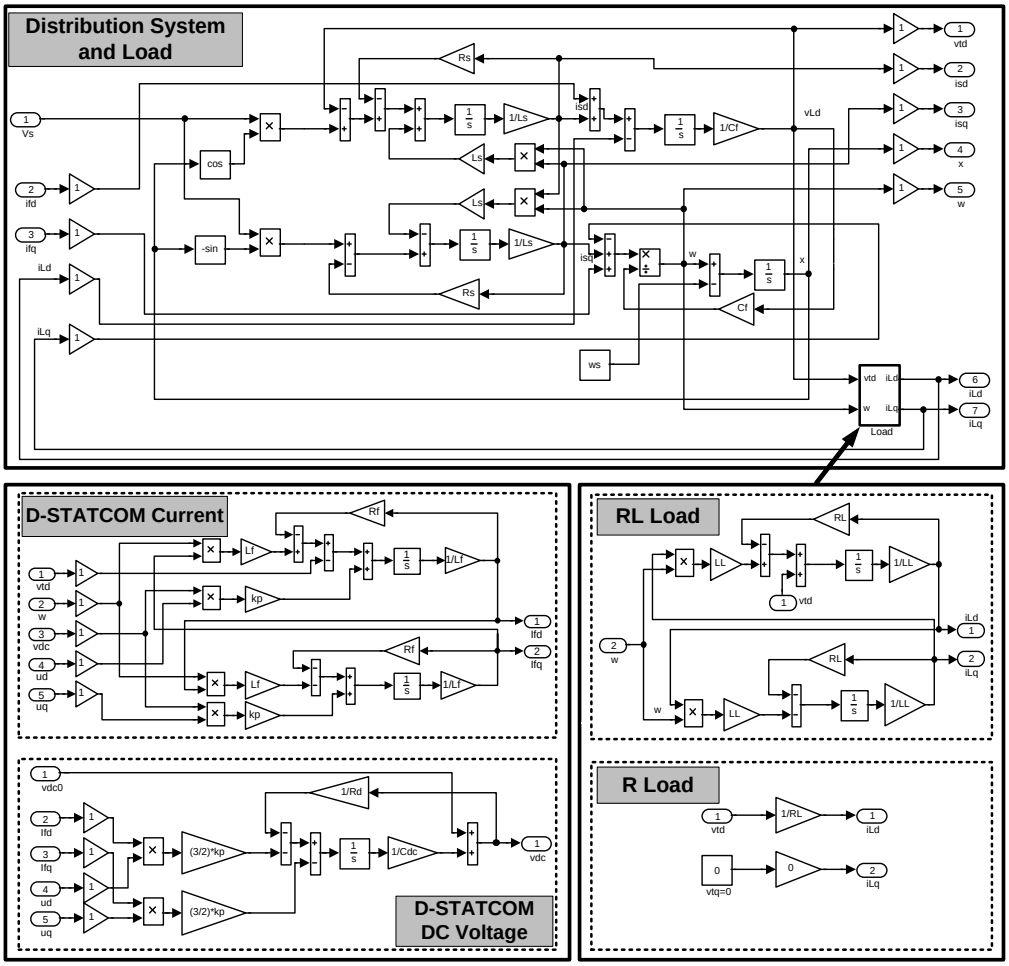

Figure 12. Test Power System and its Controllers in MATLAB Simulink

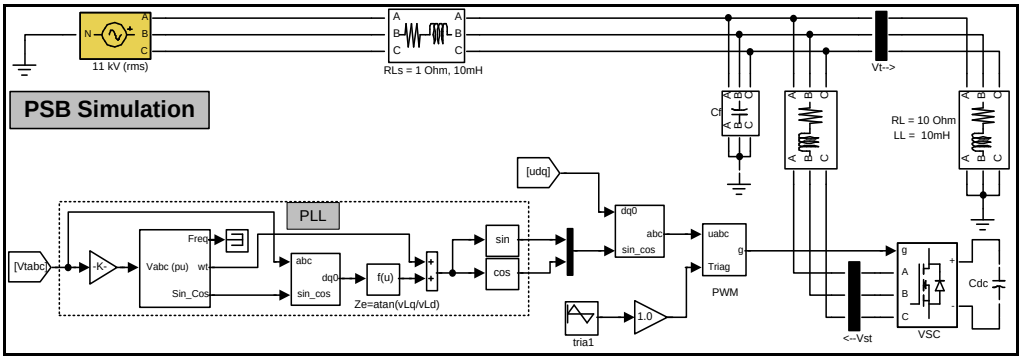

Figure 13. D-STATCOM System using MATLAB Power System Blockset (PSB)

5. Simulation Results and Discussion

The proposed D-STATCOM mathematical model, as summarized in (28), and its control were integrated with the power distribution system and the load voltage controller. This test system was formulated and therefore simulated in MATLAB

Simulink. The load voltage controller described in Section 4 provides the reactive current reference signal, i_{fq}^{*}, to the D-STATCOM controller while the active current reference signal, i_{fd}^{*}, is generated by the DC voltage controller. Other reference input to the D-STATCOM control is the desired constant DC voltage, v_{dc}^{*}.

The compensating current and DC voltage control schemes shown in Figures 5 and 6 are applied. The D-STATCOM model is integrated with the power distribution system and the load are shown in Figure 12 as created in SIMULINK/MATLAB. Simulation results for this integrated system when the source voltage are dropped to 0.9 pu., 0.8 pu. and 0.7 pu., are presented for the inductive *RL* load.

To verify the accuracy of the proposed D-STATCOM simulation, the similar task was also conducted by using MATLAB power system blockset (PSB) for simulating the D-STATCOM test system in power-electronic switching model. This can be summarized as shown in Figure 13.

With the load voltage controller designed using the classical loop shaping method, the stability margins (*i.e.*, both gain margin and phase margin) can be simply achieved to satisfy the specification. The response of the designed controller shows a good performance and preferable stability margins. Figure 14 shows the responses of the load voltage to the decreased source voltages down to 0.9 pu., 0.8 pu., and 0.7 pu., respectively. When considering the sag of the source voltage at 0.9 pu., we can see that the load voltage reaches its reference within 0.01 s. whilst the sags at 0.8 pu. and 0.7 pu. take longer time to recover, within 0.02 s.

Additionally, the responses of the load voltage control with and without the decoupling are compared. As can be seen, the load voltage controller with the decoupling gives better dynamic responses. It is because smaller settling time is experienced when the source voltage is decreased at 0.9 pu., 0.8 pu., and 0.7 pu., respective. Clearly, Figure 15 shows that the responses of the DC voltage for the D-STATCOM controllers with the decoupling also have smaller settling time and overshoot than that without the decoupling. In comparison, the simulation results show that the voltage controller with the decoupling is conservative and gives better performances.

Moreover, Figures 16 – 18 compares the dynamic responses of the load voltage, the DC voltage, and the D-STATCOM's currents of the proposed model and the PSB simulation. As a result, the responses of both simulations are thereby justifying the proposed model and the controller design.

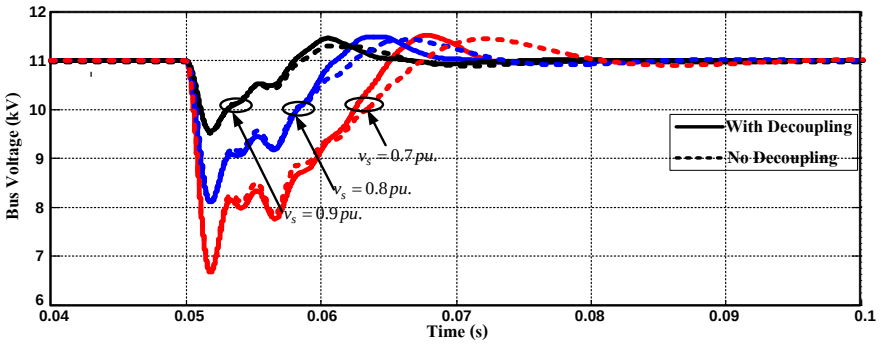

Figure 14. Load Voltage Responses

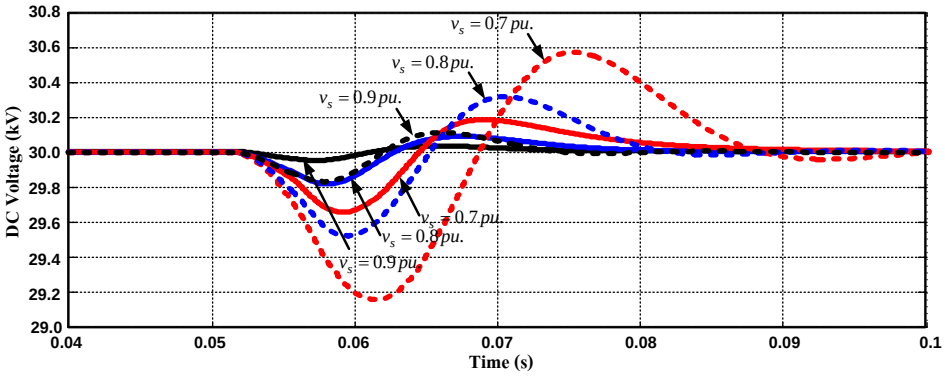

Figure 15. DC Voltage Responses

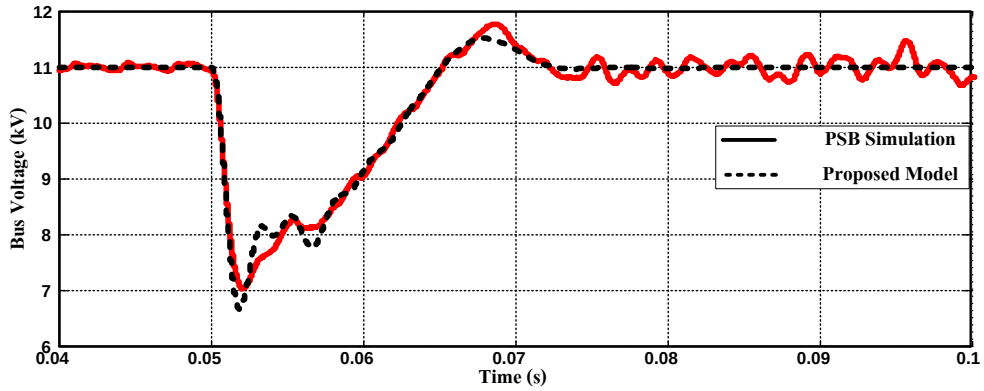

Figure 16. Comparisons for the Responses of the Load Voltage

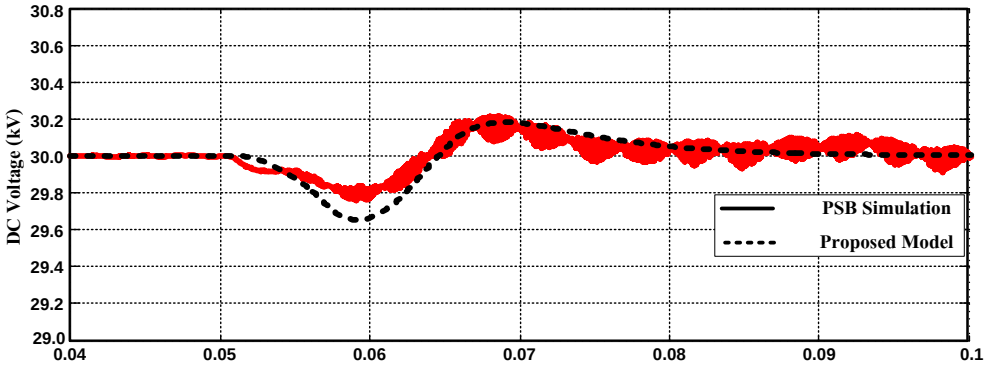

Figure 17. Comparisons for the Responses of the DC Voltage

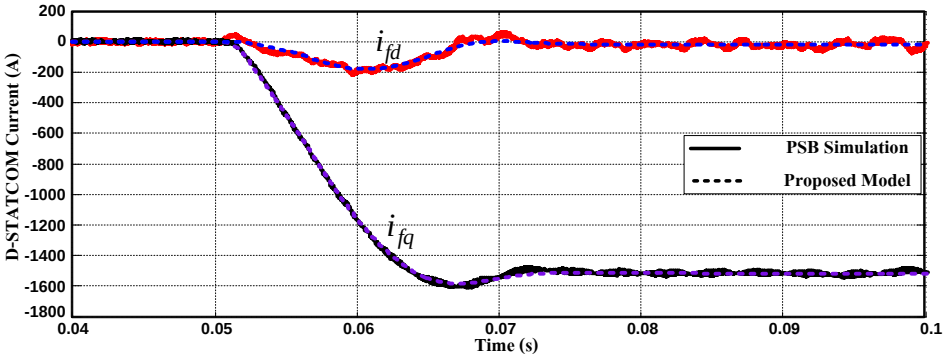

Figure 18. Comparison for the Responses of the D-STATCOM Current

6. Conclusion

This paper illustrates the system modeling and control design for the load voltage regulation using D-STATCOM. The D-STATCOM currents and DC voltage decoupling control based on the *dq* reference frame are used with the symmetrical optimum method to obtain the parameters of the PI controllers. This derived model is used for the load voltage controller design based on the linearized technique, called the classical loop shaping method. Performance of the propose model and the controller design are verified by using computer simulation performed in SIMULINK/MATLAB. The results show that the load voltage controller including the D-STATCOM controllers with the decoupling control has a good performance and sufficient stability margins. In addition, the simulation results obtained by using the proposed model in the frequency domain are compared with those acquired from MATLAB's Simulink - Power System Blockset to confirm the accuracy of this simulation.

Acknowledgements

One of the authors, Mr. Kittaya Somsai, would like to thank the office of the Higher Education Commission, Thailand for supporting a grant fund under the program Strategic Scholarships for Frontier Research Network for the Joint Ph.D Program Thai Doctoral degree for this research.

References

[1] R. C. Dugan, M. F. McGranaghan and H. Wayne Beaty, "Electrical Power System Quality", McGraw-Hill **(1996)**.
[2] A. Ghosh and G. Ledwich, "Power quality enhancement using custom power devices", Kluwer Academic, Massachusetts, **(2002)**.
[3] P. S. Sensarma, K. R. Padiya and V. Ramanarayanan, "Analysis and Performance Evaluation of a Distribution STATCOM for Compensating Voltage Fluctuations", IEEE Trans. Power Del. vol. 16, no. 2, **(2001)**, pp. 259 – 264.
[4] P. Rao, M. L. Crow and Z. Yang, "STATCOM control for power system voltage control applications", IEEE Trans. Power Del., vol. 15, no. 4, **(2000)**, pp. 1311 – 1317.
[5] K. R. Padiyar and A. M. Kulkarni, "Design of reactive current and voltage controller of static condenser", Electric Power Energy System, vol. 19, no. 6, **(1997)**, pp. 397 – 410.
[6] C. Hochgraf and R. H. Lasseter, "Statcom controls for operation with unbalanced voltages", IEEE Trans. Power Del., vol. 13, no. 2, **(1998)**, pp. 538 – 544.
[7] C. Chen and G. Joos, "Series and shunt active power conditioners for compensating distribution system faults", Canadian Conferences on Electrical Computer Engineering **(2000)** March 7 – 10, pp. 1182 – 1186.

[8] C. Schauder and H. Mehta, "Vector analysis and control of advanced static VAr compensators", IEE – Gen. Transm. Distrib., **(1993)**, pp. 299 – 306.
[9] E. Acha, V. G. Agelidis, O. Anaya-Lara and T. J. E. Miller, "Power Electronic control in Electrical system", Reed Educational and Professional, Oxford **(2002)**.
[10] C. Schauder, M. Gernhardt, E. Stacey, T. Lemak, L. Gyugyi, T. W. Cease and A. Edris, "Development of ±100 MVAr static condenser for voltage control of transmission systems", IEEE Trans. Power Del., vol. 10, no. 3, **(1995)**, pp. 1486 – 1496.
[11] W. -L. Chen, W. -G. Liang and H. -S. Gau, "Design of a mode decoupling STATCOM for voltage control of wind-driven induction generator systems", IEEE Trans. Power Del., vol. 25, no. 3, **(2010)**, pp. 1758 – 1767.
[12] M. G. Molina and P. E. Mercado, "Control design and simulation of DSTATCOM with energy storage for power quality improvements", IEEE/PES Transmission & Distribution Conf. Exposition, Latin America, TDC '06, **(2006)** August 15-18, pp. 1 – 7.
[13] G. G. Pablo and G. C. Aurelio, "Control system for a PWM-based STATCOM", IEEE Trans. Power Del., vol. 15, no. 4, **(2000)**, pp. 1252 – 1257.
[14] C. K. Sao, P. W. Lehn, M. R. Iravani and J. A. Martinez, "A benchmark system for digital time-domain simulation of a pulse-width-modulated D-STATCOM", IEEE Trans. Power Del., vol. 17, no. 4, **(2002)**, pp. 1113 – 1120.
[15] P. W. Lehn and M. R. Iravani, "Experimental evaluation of STATCOM closed loop dynamics", IEEE Trans. Power Del., vol. 13, no. 4, **(1998)**, pp. 1378 – 1384.
[16] A. Jain, K. Joshi, A. Behal and N. Mohan, "Voltage regulation with STATCOMs: modeling, control and results", IEEE Trans. Power Del., vol. 21, no. 2, **(2006)**, pp. 726 – 735.
[17] M. P. Kazmierkowski, R. Krishnan and F. Blaabjerg, "Control in power electronics selected problems", Elsevier Science, California **(2002)**.
[18] F. Frohr and F. Orttenburger, "Introduction to electronic control engineering", Second Wiley Eastern Reprint, New Delhi **(1992)**
[19] J. D'Azzo and H. Houpis, "Linear control system analysis and design: conventional and modern", McGraw-Hill, New York **(1995)**.
[20] C. Barratt and S. Boyd, "Interactive Loop-Shaping Design of MIMO Controllers", IEEE Symposium on Computer Aided Control System Design, Napa, California **(1992)** March, pp. 76 – 81.

Authors

Kittaya Somsai

Kittaya Somsai received the B.Eng degree in Electrical Engineering from Rajamangala University of Technology Thanyaburi (RMUTT) and the M.Eng degree in Electrical Engineering from King Mongkut's Institute of Technology North Bangkok (KMITNB), THAILAND in 2003 and 2005 respectively. He is currently working toward the Ph.D. degree. He is currently researching on Power System Control, Custom Power Device (CPD) and Flexible AC Transmission Systems (FACTS).

Nitus Voraphonpiput

Nitus Voraphonpiput received his B.Eng, M.Eng and Ph.D.Eng in Electrical Engineering from King Mongkut's Institute of Technology North Bangkok (KMITNB), THAILAND in 1993, 1998 and 2007 respectively. He is an engineer in charge of Power Purchase Agreement Division, Electricity Generating Authority of Thailand (EGAT). His current research interests on Power System Control and Flexible AC Transmission Systems (FACTS).

Thanatchai Kulworawanichpong

Thanatchai Kulworawanichpong is an associate professor of the School of Electrical Engineering, Institute of Engineering, Suranaree University of Technology, Nakhon Ratchasima, THAILAND. He received B.Eng. with first-class honour in Electrical Engineering from Suranaree University of Technology, Thailand (1997), M.Eng. in Electrical Engineering from Chulalongkorn University, Thailand (1999), and Ph.D. in Electronic and Electrical Engineering from the University of Birmingham, United Kingdom (2003). His fields of research interest include a broad range of power systems, power electronic, electrical drives and control, optimization and artificial intelligent techniques. He has joined the school since June 1998 and is currently a leader in Power System Research, Suranaree University of Technology, to supervise and co-supervise over 15 postgraduate students.